THE JOURNAL OF BIOLOGICAL CHEMISTRY VOL. 288, NO. 13, pp. 9272–9283, March 29, 2013
© 2013 by The American Society for Biochemistry and Molecular Biology, Inc. Published in the U.S.A.

Negative Regulation of the RalGAP Complex by 14-3-3*

Received for publication, October 7, 2012, and in revised form, January 25, 2013 Published, JBC Papers in Press, February 5, 2013, DOI 10.1074/jbc.M112.426106

Dara Leto[‡], Maeran Uhm[‡§], Anja Williams[‡], Xiao-wei Chen[‡], and Alan R. Saltiel[‡§¶1]

From the [‡]Life Sciences Institute, [§]Department of Molecular and Integrative Physiology, and [¶]Department of Internal Medicine, University of Michigan Medical School, Ann Arbor, Michigan 48109

Background: The RalGAP (GTPase-activating protein) complex (RGC) inhibits RalA activity and is negatively regulated by PI3-kinase/Akt signaling.
Results: 14-3-3 interacts with the phosphorylated RGC and inhibits its GAP function.
Conclusion: 14-3-3 modulates RalA activity by regulating the RGC.
Significance: Identifies 14-3-3 as a component of the cellular machinery that modulates RalA activity.

RGC1 and RGC2 comprise a functional RalGAP complex (RGC) that suppresses RalA activity. The PI3-kinase/Akt signaling pathway activates RalA through phosphorylation-mediated inhibition of the RGC. Here we identify a novel phosphorylation-dependent interaction between 14-3-3 and the RGC. 14-3-3 binds to the complex through an Akt-phosphorylated residue, threonine 715, on RGC2. Interaction with 14-3-3 does not alter *in vitro* activity of the GTPase-activating protein complex. However, blocking the interaction between 14-3-3 and RGC2 in cells increases suppression of RalA activity by the RGC, suggesting that 14-3-3 inhibits the complex through a non-catalytic mechanism. Together, these data show that 14-3-3 negatively regulates the RGC downstream of the PI3-kinase/Akt signaling pathway.

Members of the Ras superfamily of small GTPases translate inputs from upstream signaling pathways into biological outputs. RalA and RalB are highly homologous small GTPases that have been implicated in cell survival and proliferation (1, 2), cell migration (3), cytoskeletal rearrangements (4, 5), protein trafficking (6), glucose uptake (7), and TOR signaling (8, 9). Ral GTPases mediate their biological effects by cycling between a GDP-bound inactive conformation and GTP-bound active conformation in which they engage downstream effector proteins that regulate various cellular processes.

Ral GTPases are largely found in an inactive state in cells. However, extracellular stimuli can signal for activation of these proteins. Ral is directly activated by guanine nucleotide exchange factors (GEFs)[2] that bind to the inactive GTPase and catalyze the release of GDP so that GTP, which is ~10 times more abundant in cells than GDP (10), can bind. Two families of RalGEFs have been identified in mammalian cells. The RalGDS family contains four members (RalGDS, Rgl, Rlf/Rgl2, and Rgl3) that share sequence homology and a similar domain structure (11). These proteins are *bona fide* Ras effectors that bind to active Ras GTPases through a C-terminal Ras binding domain, thus recruiting RalGEFs to membranes where they can then activate Ral GTPases (12–14). RalA is also activated independently of Ras through RalGEFs that lack a Ras binding domain, including RalGPS1 and 2 (15), Rgr (16), and AND-34 (17). Although the physiological roles of these distinct RalGEFs are poorly understood, they may allow cells to respond to different stimuli in unique ways and provide spatial and temporal regulation of Ral GTPases (18).

The activity of Ral GTPases is also regulated by GTPase-activating proteins (GAPs), which inactivate Ral by catalyzing GTP hydrolysis. Although RalGAP activity was first reported over 20 years ago (19), our group and others (20, 21) only recently identified the proteins responsible for this activity. The RalGAP complex (RGC) consists of two proteins: a catalytic subunit (RGC2) that contains a C-terminal GAP domain with specificity for RalA and RalB and a regulatory subunit (RGC1) that stabilizes the GAP. A second RalGAP, GARNL1, shares high sequence homology with RGC2 and can also form a catalytically active complex with RGC1 (20, 21). These novel RalGAPs are only beginning to be studied, and the functional differences between RGC2 and GARNL1 are currently unknown. However, these two proteins are expressed differentially in cell and tissue types[3], suggesting that they may serve specialized roles.

We reported previously that the RGC is negatively regulated by Akt-catalyzed phosphorylation of RGC2 on multiple serine/threonine residues (20). Inhibition of the RGC by phosphorylation allows for an insulin-stimulated increase in RalA activity in adipocytes, where this small GTPase plays a critical role in Glut4 exocytosis and glucose uptake (7, 20). Thus, in this system, the RGC serves as an important regulatory point for modulation of RalA activity. Although GEFs are generally thought to serve as the primary drivers of small GTPase activation, there are multiple examples in which a GAP, either alone or in conjunction with a GEF, plays a role in activation (22). Of note, this seems to be the case for the small GTPase Rheb, which is activated by hormone signaling through inhibition of the tuberous sclerosis complex (TSC), a GAP complex that has a striking

* This work was supported, in whole or in part, by National Institutes of Health Grant DK076906 (to A. R. S.).
[1] To whom correspondence should be addressed: Life Sciences Institute, University of Michigan, 210 Washtenaw Ave., Ann Arbor, MI 48109. Tel.: 734-615-9787; Fax: 734-763-6492; E-mail: saltiel@umich.edu.
[2] The abbreviations used are: GEF, guanine nucleotide exchange factor; GAP, GTPase-activating protein; RGC, RalGAP complex; GDS, GDP dissociation stimulator; TSC, tuberous sclerosis complex; DIG, digoxigenin; pAS, phospho-Akt substrate; DN, dominant-negative.
[3] D. Leto, M. Uhm, A. Williams, and A. R. Saltiel, unpublished observation.

similarity to the RGC (21, 23–26). Thus, at least in some cases, relieving negative regulation by a GAP appears to be necessary for the activation of the target small GTPase.

Phosphorylation-induced inhibition of GAPs can occur through direct inactivation of catalytic activity or through indirect mechanisms, such as altering the interactions of the GAP with other proteins, stability, or localization (22, 27). Members of the 14-3-3 family of proteins bind to some phosphorylated GAPs and GEFs and modulate their function (28–30). 14-3-3s take on many roles in signaling pathways by binding to hundreds of phosphorylated proteins and regulating their function. Mammalian cells ubiquitously express seven 14-3-3 isoforms (β, ϵ, γ, η, θ, σ, and ζ) that recognize and dock to target proteins through phosphoserine or phosphothreonine residues within an R*XX*pS/T*X*P motif (mode 1 binding) or an R*X*(F/Y)*X*pS*X*P motif (mode 2 binding) (31). Here we report that Akt-catalyzed phosphorylation of RGC2 increases 14-3-3 binding to the RGC and that this interaction inhibits RGC function in cells. These data establish a role for 14-3-3 in hormone-stimulated activation of RalA.

EXPERIMENTAL PROCEDURES

DNA Constructs—The FLAG-RalA and HA-RGC1 constructs were described previously (7, 20). The RGC1 shRNA-resistant construct (HA-RGC1^{res}) was generated by site-directed mutagenesis using the following primer: 5′-GGAGTGGCATGGCCCAACAGATCGCTTACGAAATTCACCTTGAGC-3′. The human FLAG-RGC2 construct was obtained from Origene Technologies, Inc. The RGC2 T715A point mutation was introduced by site-directed mutagenesis using the following primer: 5′-ATGCGATTTAGGAGTGCCGCCACGTCTGGAGCACCGGG-3′. The rat 14-3-3ϵ cDNA and human 14-3-3β cDNA were provided by Dr. Ken Inoki (University of Michigan) and subcloned into a pKH3 (7) vector. The human cDNAs for all other 14-3-3 isoforms were purchased from Open Biosystems (14-3-3γ, clone identification no. 3915246; 14-3-3η, clone identification no. LIFESEQ2207186; 14-3-3θ, clone identification no. 6164592; 14-3-3σ, clone identification no. 3445915; and 14-3-3ζ, clone identification no. 5563061) and subcloned into the pKH3 and pGEX-4T-1 vectors. The 14-3-3θ R56/60A dominant-negative construct was generated by site-directed mutagenesis using the following primer: 5′-GTGGTCGGGGGCCGCGCGTCCGCCTGGGCGGTCATCTCTAGCATC-3′. DNA sequencing was performed at the University of Michigan DNA Sequencing Core.

Antibodies—The rabbit IgG, mouse IgG, and anti-FLAG mouse antibodies were purchased from Sigma-Aldrich. The anti-digoxigenin (DIG) HRP-conjugated mouse antibody was purchased from Roche. The anti-Akt rabbit, anti-phospho-Akt Ser-473 rabbit, anti-phospho-14-3-3 binding site mouse, and phospho-Akt substrate rabbit antibodies were purchased from Cell Signaling Technology. The anti-HA mouse and anti-14-3-3 rabbit and mouse antibodies were purchased from Santa Cruz Biotechnology. The anti-RalA mouse antibody was purchased from BD Biosciences. The anti-RGC1, anti-RGC2, anti-RGC2 pS486, anti-RGC2 pS696, and anti-RGC2 pT715 rabbit antibodies were described previously (20).

Cell Culture, Transfections, and Inhibitors—293T and 293A cells were maintained as described previously (32). 3T3-L1 fibroblasts were maintained and differentiated as described previously (32). 293T and 293A cells were transfected using Lipofectamine 2000 reagent (Invitrogen) according to the protocol of the manufacturer and harvested 48 h after transfection. 3T3-L1 adipocytes were transfected by electroporation as described previously (33). Cells were pretreated with 100 nM wortmannin (Sigma-Aldrich) for 1 h or 1 μM Akti-1/2 (Calbiochem) for 2 h before addition of insulin (Sigma-Aldrich).

Lentiviral constructs encoding a shRNA control sequence (Open Biosystems) or a shRNA sequence that targets RGC1 (Open Biosystems, clone identification no. V2LHS_32227) were obtained from the University of Michigan Vector Core Facility. 293T cells were transfected with shRNA constructs as described above. 48 h after transfection, cells stably expressing the shRNA were selected by culturing in DMEM supplemented with 10% FBS and 2 μg/ml puromycin. The medium was replaced every 3 days, and after 2 weeks the GFP-positive population of cells was collected by FACS (University of Michigan Flow Cytometry Core). Stably transfected cells were maintained in DMEM supplemented with 10% FBS and 0.5 μg/ml puromycin.

Protein Purification—GST proteins were induced and purified as described previously (34). Purified GST-14-3-3θ was eluted from glutathione beads by washing the beads with 10 mM glutathione in PBS (pH 8.0). The elution was monitored by A_{280} readings, and fractions containing protein were pooled and dialyzed overnight against 4 liters of ice-cold PBS. The proteins were then concentrated using an Amicon centrifugal filtration unit (Millipore). Concentrated proteins were stored at −80 °C in PBS containing 10% glycerol and 10 mM DTT.

Immunoprecipitations, Pull-downs, and Western Blotting—Unless noted otherwise, the 14-3-3θ isoform was used for all experiments. For immunoprecipitations, cells were washed twice with ice-cold PBS before lysis in 1 ml of 14-3-3 immunoprecipitation buffer (IP buffer; 10 mM Tris-HCl (pH 7.5), 100 mM NaCl, 1% Nonidet P-40, 1% TX-100, 50 mM NaF, 2 mM EDTA) supplemented with an EDTA-free protease inhibitor tablet (Roche). Lysates were cleared by centrifuging at 13,000 × *g* for 10 min and then incubated with 5 μg of antibody for 4 h at 4 °C. For the last 2 h, protein A/G beads (Santa Cruz) were added to precipitate the antibody. Beads were washed three times with IP buffer and then resuspended in 2× SDS sample buffer.

For 14-3-3 pull-downs, cells were washed once with ice-cold PBS and then lysed in 1 ml of 14-3-3 pull-down buffer (PD buffer; 15 mM Tris-HCl (pH 7.5), 150 mM NaCl, 0.5% Nonidet P-40, 1 mM DTT) supplemented with an EDTA-free protease inhibitor tablet (Roche). Lysates were cleared by centrifuging at 13,000 × *g* for 10 min and then incubated with 10 μg of GST or GST-14-3-3θ bound to glutathione beads (GE Healthcare) for 1.5 h at 4 °C. For samples treated with phosphatase, lysates were preincubated with 5000 units of λ-phosphatase (New England Biolabs, Inc.) at 30 °C or 500 units of calf intestinal phosphatase (New England Biolabs, Inc.) at 37 °C for 1 h before adding GST-14-3-3 beads. Beads were washed three times with 1 ml of PD

buffer and then resuspended in 2× SDS sample buffer. RalA activation assays were performed as described previously (7).

Samples were resolved by SDS-PAGE. SDS-PAGE gels were transferred to nitrocellulose membranes. Membranes were incubated with the indicated primary antibodies and horseradish peroxidase secondary antibodies (Pierce) before reacting with ECL Western blotting substrate (Pierce). Western blot analyses were quantified by densitometry using ImageJ.

Preparation of DIG-labeled Proteins and Overlay Assay—GST or GST-14-3-3θ was labeled with DIG by incubating 25 μg of protein with 30 μM digoxigenin-3-*O*-methylcarbonyl-ε-aminocaproic acid-*N*-hydroxysuccinimide ester (Roche) in 350 μl of PBS for 15 min at room temperature. The labeling reaction was stopped by adding 100 μl of 1 M Tris-HCl (pH 7.5). Labeled protein was dialyzed against 1 liter of 25 mM Tris-HCl (pH 7.5) for 1 h at room temperature, then against 4 liters of PBS (pH 7.4) for 4 h at 4 °C, and finally against 4 liters of fresh PBS (pH 7.4) for 16 h at 4 °C. Labeled protein was then diluted in 25 ml of TBS (50 mM Tris-HCl (pH 7.5), 150 mM NaCl) containing 2 mg/ml BSA (Sigma-Aldrich) and 0.01% sodium azide (Sigma-Aldrich). DIG-labeled proteins were stored at 4 °C.

For overlay assays, the RGC was immunoprecipitated from 293T cells or 3T3-L1 adipocytes and resolved by SDS-PAGE. Proteins were transferred to a nitrocellulose membrane. The membrane was blocked at room temperature overnight in blocking buffer (5% skim milk in TBS-Tween). The membrane was incubated with DIG-labeled proteins for at least 4 h at 4 °C and then washed three times with TBS-T. The membrane was incubated with blocking buffer containing anti-DIG HRP antibody (1:10,000, Roche) for 2 h at room temperature and washed three times with TBS-T. Overlays were visualized by reacting with ECL Western blotting substrate (Pierce).

λ-Phosphatase Protection Assay—293T cells were lysed in 1 ml of PD buffer supplemented with 50 mM NaF, and overexpressed RGC was immunoprecipitated from cleared lysates using an anti-FLAG antibody conjugated to agarose beads. Beads were washed three times with 1 ml of PD buffer containing NaF and two times with 1 ml of PD buffer without NaF. The beads were incubated with or without 10 μg of GST-14-3-3θ for 1 h at 4 °C and then washed five times with 1 ml of PD buffer without NaF. The beads were then resuspended in 250 μl of PD buffer without NaF supplemented with 1 mM $MnCl_2$. Beads were equilibrated to 30 °C, and then 800 units of λ-phosphatase was added to each sample. To stop the reaction, 50 μl of the reaction was removed at the indicated time points and placed into a chilled Eppendorf tube containing 5× SDS sample buffer.

GAP Assay and Kinase Assay—The protocols used for GAP assays and kinase assays were described previously (20). For the GAP assay containing GST-14-3-3, RGC1/2 was prebound to 14-3-3 as described above.

RESULTS

Identification of 14-3-3 as a RalGAP Complex-interacting Protein—The 14-3-3 recognition motifs (R*XX*pS/T*X*P and R*X*(F/Y)*X*pS*X*P) coincide with sequences that are phosphorylated by AGC kinase members, and there are numerous examples that demonstrate roles for 14-3-3 proteins in modulating signaling downstream of AGC kinases (29, 35–39). On the basis of our recent finding that the RGC is negatively regulated by Akt-catalyzed phosphorylation of RGC2 (20), we hypothesized that 14-3-3 may interact with the RGC.

We investigated whether the RGC was a putative 14-3-3 binding partner by immunoprecipitating the endogenous complex from 3T3-L1 adipocytes treated with or without insulin and immunoblotting with an antibody that detects phosphorylated residues that lie within a 14-3-3 binding site motif (p14-3-3 binding site antibody, Fig. 1*A*). As shown previously (20), both the RGC1 and RGC2 subunits of the complex were immunoprecipitated using an anti-RGC2 antibody, whereas the complex was absent from a control immunoprecipitation using rabbit IgG antibody. The p14-3-3 binding site antibody weakly detected a band corresponding to the molecular weight of RGC2 in the RGC2 immunoprecipitation (Fig. 1*A*, *arrow*). Detection of RGC2 by this phospho-antibody was enhanced when the complex was immunoprecipitated from lysates treated with insulin. RGC2 phosphorylation that was detected by the p14-3-3 binding site antibody was maximal by 2 min after insulin stimulation and was sustained for up to 90 min after stimulation (Fig. 1*B*). Phosphorylation was increased by insulin in a dose-dependent manner that correlated with activation of Akt, which we previously showed catalyzes RGC2 phosphorylation on multiple residues (20) (Fig. 1*C*). To test whether the phospho-14-3-3 binding site antibody detects Akt-catalyzed phosphorylation, we immunoprecipitated the RGC from 3T3-L1 adipocyte lysates that were pretreated with the PI3-kinase inhibitor wortmannin or the Akt inhibitor Akti-1/2 before stimulation with insulin. Both inhibitors blocked RGC2 detection by the phospho-14-3-3 binding site antibody (Fig. 1*D*). Together, these data raised the possibility that 14-3-3 may recognize a residue or residues on RGC2 that are phosphorylated by Akt in response to insulin.

Next, we tested whether 14-3-3 binds to the RGC. We found that although endogenous 14-3-3 was not detected in an immunoprecipitation using control mouse IgG, 14-3-3 coimmunoprecipitated with overexpressed RGC in 293T cells (Fig. 2*A*, *left panel*). The reciprocal immunoprecipitation confirmed that 14-3-3 interacts with the RGC (Fig. 2*A*, *right panel*). We also detected endogenous 14-3-3 in an immunoprecipitation of endogenous RGC2 from 3T3-L1 adipocytes (Fig. 2*B*). More 14-3-3 was detected in complex with RGC2 when cells were treated with insulin, demonstrating that this interaction is subject to hormonal regulation.

Seven highly homologous isoforms of 14-3-3 are ubiquitously expressed in mammalian cells. To determine whether there was isoform-specific binding between 14-3-3s and the RGC, we transfected 3T3-L1 adipocytes with HA-tagged 14-3-3 proteins and probed their interaction with the endogenous RGC. Immunoprecipitation of HA-14-3-3 β, ε, η, and θ coimmunoprecipitated the RGC, with 14-3-3θ showing the most interaction, whereas HA-14-3-3 γ, σ, and ζ displayed little to no interaction (Fig. 2*C*). Furthermore, stimulation with insulin once again significantly increased binding between 14-3-3 and the RGC (Fig. 2*C*, compare *sixth* and *ninth lanes*).

We investigated whether this interaction requires RGC1, RGC2, or both subunits of the complex. To test the binding between 14-3-3 and the individual subunits of the complex, we

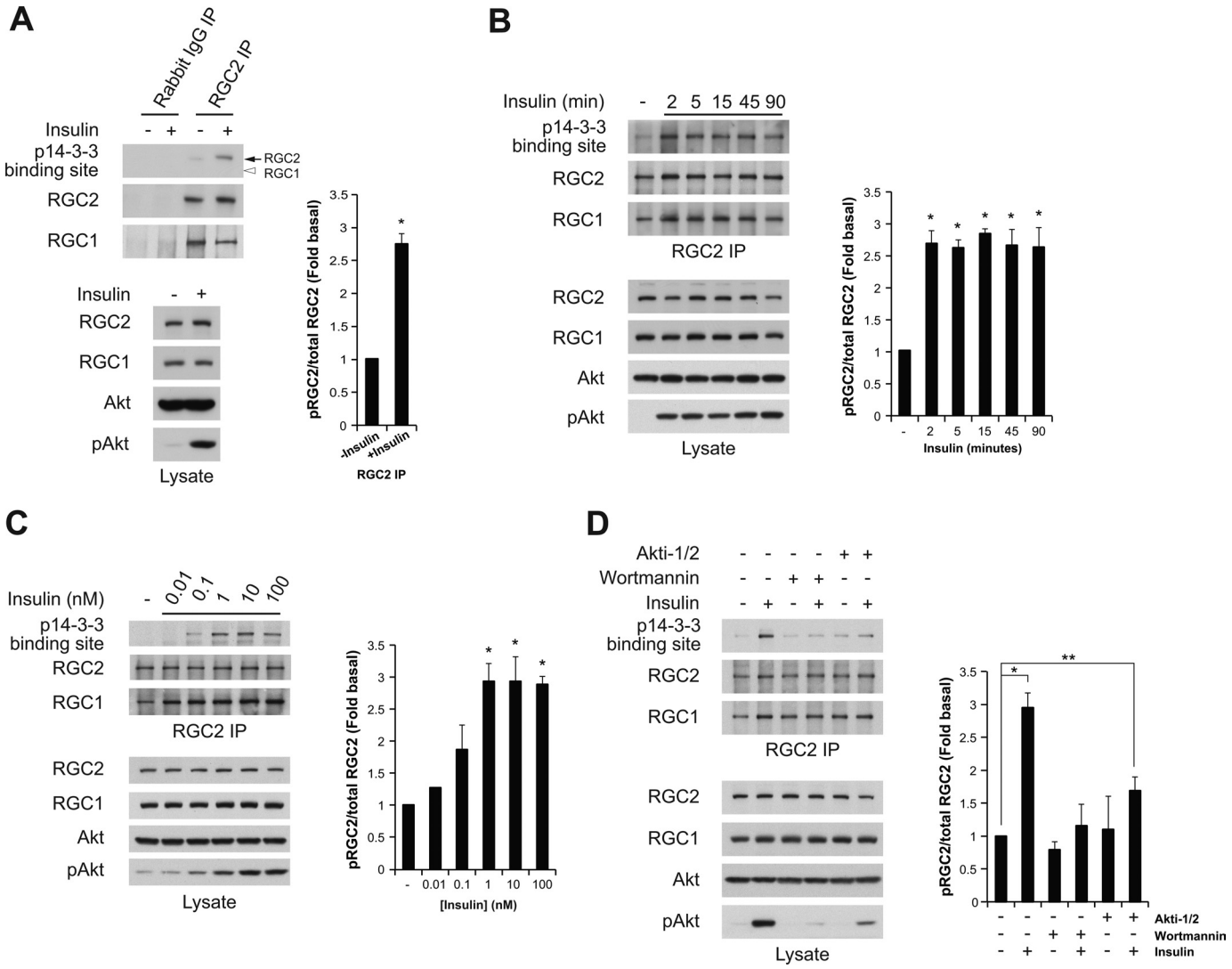

FIGURE 1. **The RalGAP complex contains a 14-3-3 recognition motif.** *A*, serum-starved 3T3-L1 adipocytes were mock-treated or stimulated with 100 nM insulin for 15 min before lysis. Lysates were immunoprecipitated (*IP*) with control rabbit IgG or anti-RGC2 antibody. The immune complexes and cell lysates were resolved by SDS-PAGE before Western blotting with the indicated antibodies. The *arrowhead* and *arrow* indicate the relative positions of RGC1 and RGC2, respectively. *Left panel*, Western blot analysis. *Right panel*, phospho-RGC2 and total RGC2 signals in the RGC2 immunoprecipitations were quantified and normalized to the basal signal. The normalized phospho-RGC2/total RGC2 ratio is presented as the mean ± S.E. of three independent experiments. *, $p < 0.02$, Student's *t* test. *B*, serum-starved 3T3-L1 adipocytes were mock-treated or stimulated with 100 nM insulin for the indicated times before lysis. The RGC was immunoprecipitated from lysates using the anti-RGC2 antibody. The immune complexes and cell lysates were resolved by SDS-PAGE followed by Western blotting with the indicated antibodies. *Left panel*, Western blot analysis. *Right panel*, quantification was performed as described in *A*. *Error bars* represent mean ± S.E. of three independent experiments. *, $p < 0.02$, Student's *t* test. *C*, serum-starved 3T3-L1 adipocytes were mock-treated or stimulated with the indicated doses of insulin for 15 min before lysis. The RGC was immunoprecipitated from lysates using the anti-RGC2 antibody. The immune complexes and cell lysates were resolved by SDS-PAGE and subjected to Western blot analysis with the indicated antibodies. *Left panel*, Western Blot analysis. *Right panel*, quantification was performed as described in *A*. *Error bars* represent mean ± S.E. of three independent experiments. *, $p < 0.02$, Student's *t* test. *D*, serum-starved 3T3-L1 adipocytes were treated with 100 nM wortmannin for 1 h or 1 μM Akti-1/2 for 2 h before mock treatment or stimulation with insulin for 15 min. The RGC was immunoprecipitated from cell lysates using the anti-RGC2 antibody. Immune complexes and cell lysates were resolved by SDS-PAGE followed by Western blot analysis with the indicated antibodies. *Left panel*, Western blot analysis. *Right panel*, quantification was performed as described in *A*. *Error bars* represent mean ± S.E. of three independent experiments. *, $p < 0.02$; **, $p < 0.05$, Student's *t* test.

created a cell line that is depleted of the endogenous complex and then reintroduced the subunits of the complex individually or in conjunction with one another. Because 293T cells express undetectable levels of endogenous RGC2[3], RGC1 was knocked down by stably transfecting cells with anti-RGC1 shRNA. Expression of RGC1 was reduced by 71% using this method (Fig. 2*D*). Wild-type HA-RGC1 was also knocked down in these cells. However, expression was recovered when shRNA-resistant HA-RGC1 (HA-RGC1^{res}) was transfected into cells (Fig. 2*D*). Thus, using this cell line, we were able to dissect the interaction between 14-3-3 and overexpressed RGC1 and RGC2 with minimal expression of endogenous RGC proteins.

The interaction between 14-3-3 and subunits of the RGC was explored through overlay and pull-down assays. In an overlay assay, 14-3-3 bound to FLAG-RGC2 (Fig. 2*E*, *arrow*, *third* and *fourth lanes*) but not to HA-RGC1 (Fig. 2*E*, *arrowheads*, *second* and *fourth lanes*), demonstrating that 14-3-3 binds directly to the RGC through RGC2 in an *in vitro* setting. Next, a pull-down assay was used to interrogate the interaction in cells. In contrast

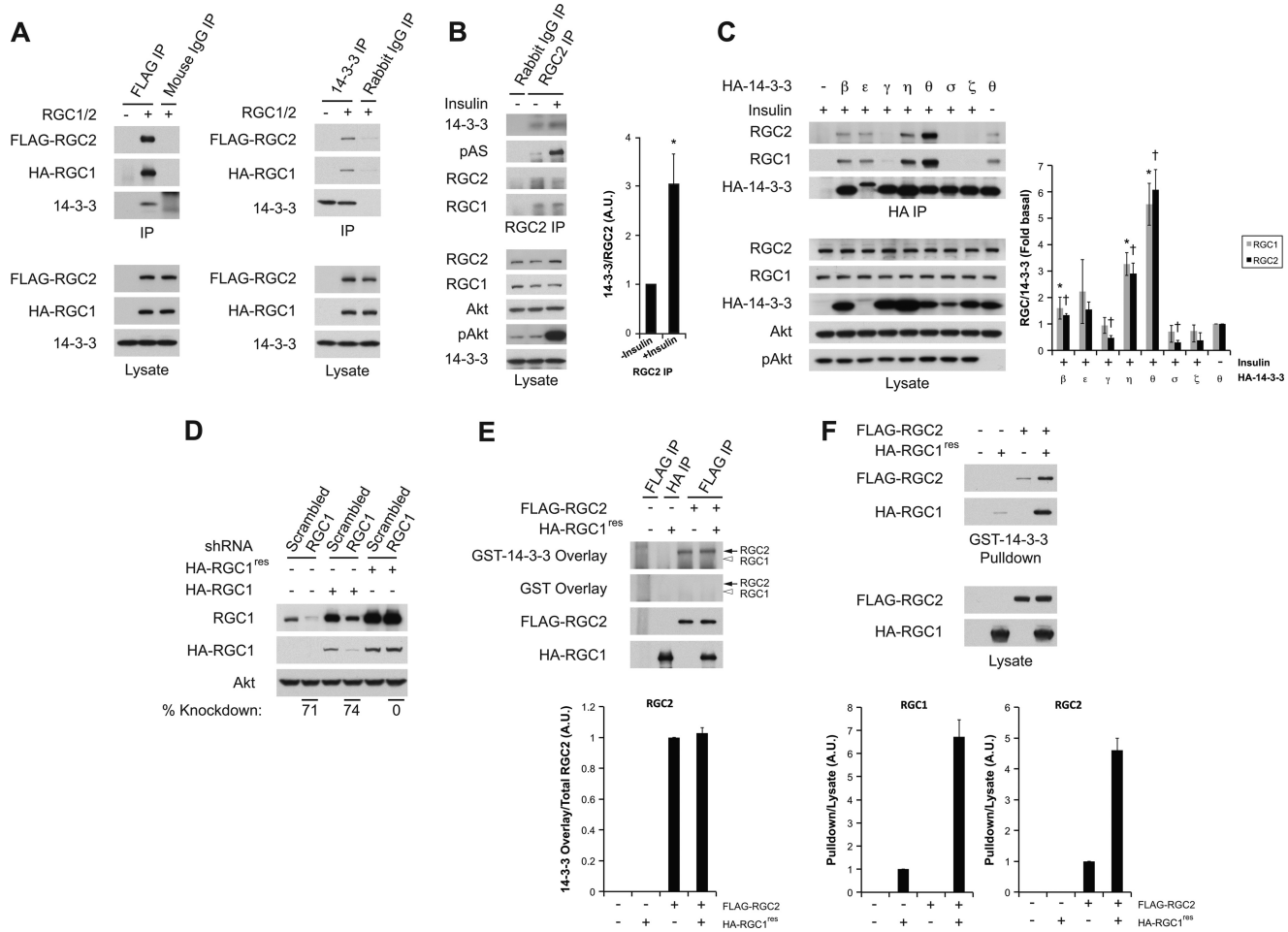

FIGURE 2. **14-3-3 interacts with the RalGAP complex.** *A*, 293T cells were transfected with empty vector or HA-RGC1 and FLAG-RGC2 as indicated. Two days after transfection, cell lysates were subjected to immunoprecipitation (*IP*) using anti-FLAG antibody (*left panel*) or anti-14-3-3 antibody (*right panel*). Immune complexes and lysates were resolved by SDS-PAGE and analyzed by Western blotting with the indicated antibodies. *B*, serum-starved 3T3-L1 adipocytes were mock-treated or stimulated with 10 nM insulin for 15 min before lysis. Lysates were subjected to immunoprecipitation using an anti-RGC2 antibody. The immune complexes and cell lysates were resolved by SDS-PAGE and visualized by Western Blot analysis using the indicated antibodies. *Left panel*, Western blot analysis. *Right panel*, 14-3-3 and RGC2 signals in the RGC2 immunoprecipitation were quantified and normalized to the basal signal. The normalized 14-3-3/RGC2 ratio is presented as the mean ± S.E. of three independent experiments. *, $p < 0.03$, Student's *t* test. *A.U.*, arbitrary unit. *C*, 3T3-L1 adipocytes were transfected with empty vector or the indicated HA-tagged 14-3-3 isoforms. One day after transfection, cells were serum-starved for 4 h before mock treatment or stimulation with 100 nM insulin for 15 min. Lysates were subjected to immunoprecipitation using an anti-HA antibody. Immune complexes and lysates were resolved by SDS-PAGE and analyzed by Western blot analysis with the indicated antibodies. *Left panel*, Western blot analysis. *Right panel*, RGC1, RGC2, and HA-14-3-3 signals in the HA immunoprecipitation were quantified and normalized to the basal signal. The normalized RGC1/HA-14-3-3 and RGC2/HA-14-3-3 ratios are presented as the mean ± S.E. from three independent experiments. * and † $p < 0.05$, Student's *t* test. *D*, 293T cells were stably transfected with control shRNA or shRNA targeting RGC1. Control and RGC1 knockdown cells were then transiently transfected with either wild-type or shRNA-resistant HA-RGC1 (*HA-RGC1^{res}*). Cell lysates were harvested 2 days after transfection. Knockdown of endogenous RGC1 protein and recovery with the HA-RGC1 constructs were assessed by Western blot analysis with the indicated antibodies. Percent knockdown was determined from the ratio of the RGC1 signal in knockdown and control cells (knockdown/control signal × 100). Values represent the mean from three independent experiments. *E*, RGC1 knockdown cells were transfected with empty vector, HA-RGC1 alone, FLAG-RGC2 alone, or both HA-RGC1 and FLAG-RGC2. Two days after transfection, overexpressed proteins were immunoprecipitated from cell lysates using anti-HA antibody or anti-FLAG antibody. The immunoprecipitated proteins were separated by SDS-PAGE, and immunoprecipitation efficiency was assessed by Western blot analysis with the indicated antibodies. *In vitro* binding between 14-3-3 and RGC1 (*arrowhead*) or RGC2 (*arrow*) was assessed by overlay using either DIG-labeled GST or GST-14-3-3 followed by incubation with anti-DIG HRP antibody. *Top panel*, Western blot analysis. *Bottom panel*, the GST-14-3-3 overlay signal and FLAG-RGC2 signal were quantified and normalized to the signal in the *third lane*. The normalized 14-3-3 overlay/total RGC2 ratio is represented as mean ± S.E. of two independent experiments. *F*, RGC1 knockdown cells were transfected as in *E*. Cell lysates were incubated with GST-14-3-3 conjugated to glutathione beads for 90 min. Pull-down samples were resolved by SDS-PAGE and analyzed by Western blot analysis with the indicated antibodies. *Top panel*, Western blot analysis. *Bottom panel*, RGC1 and RGC2 signals in the pull-downs and lysates were quantified and normalized to the *second lane* for RGC1 and the *third lane* for RGC2. The normalized pull-down/lysate ratio is represented in arbitrary units. *Error bars* represent mean ± S.E. of three independent experiments.

to the *in vitro* data, 14-3-3 minimally bound to HA-RGC1 or FLAG-RGC2 when expressed alone in cells (Fig. 2*F*, *second* and *third lanes*, respectively). However, when the subunits were coexpressed, the amount of the complex that was pulled down by 14-3-3 was increased significantly (Fig. 2*F*, *fourth lane*). The apparent inconsistency in these findings was somewhat surprising. However, there are several possible reasons why RGC1 may be required for efficient recognition of the RGC by 14-3-3 in cells, although the binding appears to occur through RGC2. We showed previously that RGC1 acts as a regulatory subunit by stabilizing RGC2 (20), raising the possibility that RGC2 is mislocalized or takes on a conformation that occludes 14-3-3 binding in the absence of RGC1. Together, these data show that although binding between 14-3-3 and the RGC occurs through

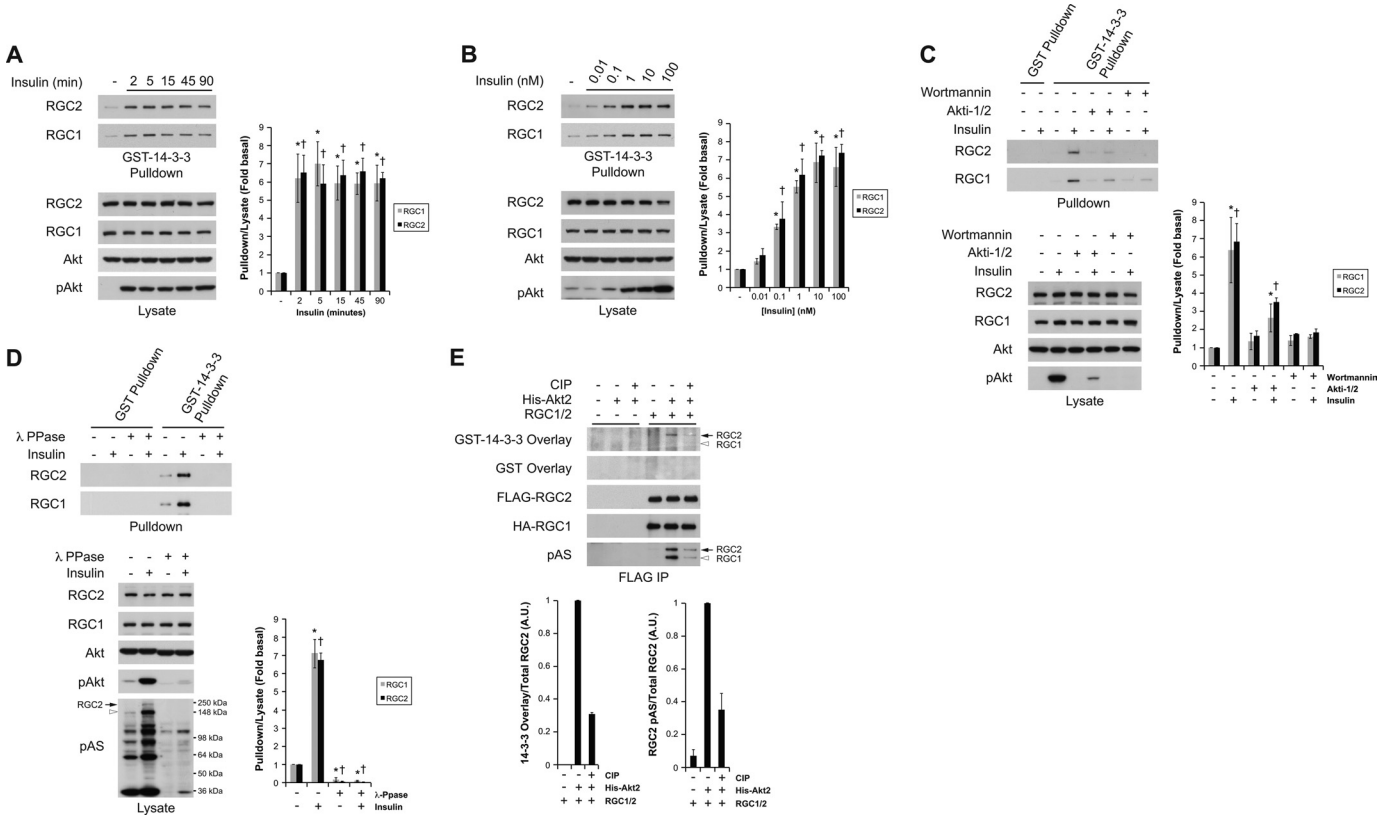

FIGURE 3. **14-3-3 binding to the RalGAP complex requires Akt-catalyzed phosphorylation.** *A*, serum-starved 3T3-L1 adipocytes were mock-treated or stimulated with 100 nM insulin for the indicated times before lysis. Lysates were incubated with GST-14-3-3 bound to glutathione beads for 90 min. Pull-downs and lysates were resolved by SDS-PAGE and analyzed by Western blotting with the indicated antibodies. *Left panel*, Western blot analysis. *Right panel*, RGC1 and RGC2 signals in the pull-down and lysates were quantified and normalized to the basal signal. The normalized pull-down/lysate ratio is presented as the mean ± S.E. of four independent experiments. * and †, $p < 0.02$, Student's *t* test. *B*, serum-starved 3T3-L1 adipocytes were mock-treated or stimulated with the indicated doses of insulin for 15 min before lysis. Pull-downs were performed and analyzed as described in *A*. *Left panel*, Western blot analysis. *Right panel*, quantification was performed as described in *A*. *Error bars* represent mean ± S.E. from three independent experiments. *, $p < 0.04$; †, $p < 0.02$, Student's *t* test. *C*, 3T3-L1 adipocytes were serum-starved before the addition of 1 μM Akti-1/2 for 2 h or 100 nM wortmannin for 1 h. After treatment with the inhibitors, the cells were mock-treated or stimulated with 100 nM insulin for 15 min and then lysed. Pull-downs were performed and analyzed as described in *A*. *Left panel*, Western blot analysis. *Right panel*, quantification was performed as described in *A*. *Error bars* represent mean ± S.E. from three independent experiments. *, $p < 0.04$; †, $p < 0.02$, Student's *t* test. *D*, serum-starved 3T3-L1 adipocytes were mock-treated or stimulated with 100 nM insulin for 15 min before lysis. Lysates were treated with or without λ-phosphatase for 1 h and then subjected to pull-down. Pull-downs were performed and analyzed as described in *A*. The relative positions of RGC1 (*arrowhead*) and RGC2 (*arrow*) are indicated in the pAS Western blot analysis. *Left panel*, Western blot analysis. *Right panel*, quantification was performed as described in *A*. *Error bars* represent mean ± S.E. from three independent experiments. * and †, $p < 0.01$, Student's *t* test. *E*, 293A cells were transfected with empty vector or HA-RGC1 and FLAG-RGC2 as indicated. Two days after transfection, cell lysates were subjected to immunoprecipitation (*IP*) using anti-FLAG antibody. The immunoprecipitated proteins were then phosphorylated *in vitro* by incubating with ATP and recombinant His-Akt2. The kinase was then removed by washing, and the immunoprecipitated proteins were incubated with or without calf intestinal phosphatase for 1 h. Immunoprecipitated proteins and lysates were resolved by SDS-PAGE, and total protein amounts and phosphorylation of the RGC was determined by Western blot analysis with the indicated antibodies. 14-3-3 binding to RGC1 (*arrowhead*) or RGC2 (*arrow*) was assessed by overlay using DIG-labeled GST or GST-14-3-3 followed by incubation with anti-DIG HRP antibody. *Top panel*, Western blot analysis. *Bottom panel*, the GST-14-3-3 overlay, pAS, and FLAG-RGC2 signals in the FLAG immunoprecipitation were quantified, and the normalized ratios of 14-3-3 overlay/total RGC2 and pAS/total RGC2 were calculated. *Error bars* represent mean ± S.E. of two independent experiments. *CIP*, calf intestinal phosphatase; *A.U.*, arbitrary unit.

a direct interaction with RGC2, both subunits are required for recognition of the complex by 14-3-3 in cells.

14-3-3 Binding Requires RGC2 Phosphorylation—To determine whether RGC phosphorylation is required for its recognition by 14-3-3, we analyzed the interaction between these proteins in 3T3-L1 adipocytes treated with insulin. Stimulation with insulin increased the amount of the RGC that interacted with GST-14-3-3 in a pull-down assay by ~6.5-fold (Fig. 3, *A–D*). This increase in binding was evident by 2 min and was sustained up to 90 min after insulin treatment (Fig. 3*A*), consistent with the increase in recognition of RGC2 by the p14-3-3 binding site antibody (Fig. 1*B*). Likewise, the association between GST-14-3-3 and the RGC increased in an insulin dose-dependent manner (Fig. 3*B*), consistent with the dose-dependent increase in recognition of RGC2 by the p14-3-3 binding site antibody (Fig. 1*C*). To investigate whether this association is dependent on Akt, we pretreated 3T3-L1 adipocytes with wortmannin or Akti-1/2 before stimulation with insulin. Pretreatment with either inhibitor decreased recognition of the RGC by 14-3-3 (Fig. 3*C*). Furthermore, as wortmannin inhibited Akt activation to a greater extent than Akti-1/2 (Fig. 3*C*, *Lysate*), it also resulted in a larger block in 14-3-3 binding (*Pull-down*), providing further evidence that Akt activation is required for this interaction.

To directly test whether Akt-catalyzed phosphorylation is required for 14-3-3 binding, we first treated 3T3-L1 lysates with λ-phosphatase to decrease total phosphorylation levels. λ-Phosphatase greatly decreased basal and insulin-stimulated

Akt phosphorylation and phosphorylation of protein targets downstream of Akt, including RGC2, as measured using the phospho-Akt substrate (pAS) antibody (Fig. 3*D*, *arrow*). λ-Phosphatase treatment also abolished phosphorylation of a protein running at the approximate molecular weight of RGC1 (Fig. 3*D*, *arrowhead*). However, because RGC1 is roughly the same size as the Akt target AS160, we cannot distinguish phosphorylation of these two proteins in cell lysates blotted with the pAS antibody.

When lysates from insulin-treated cells were subjected to pull-down using immobilized GST-14-3-3, lysates that were not preincubated with λ-phosphatase showed an insulin-dependent increase in the interaction between the RGC and 14-3-3 (Fig. 3*D*, *Pull-down*, *fifth* and *sixth lanes*). Treatment with λ-phosphatase completely abolished recognition of the RGC by 14-3-3 in the absence or presence of insulin, demonstrating that phosphorylation of RGC2 is indeed required for 14-3-3 binding (Fig. 3*D*, *Pull-down*, *seventh* and *eighth lanes*).

Although these data strongly support a role for Akt-catalyzed phosphorylation in recognition of the complex by 14-3-3, they do not rule out a role for other protein kinases that may phosphorylate the complex downstream of PI3-kinase. Thus, we explored whether phosphorylation by Akt is sufficient for 14-3-3 binding to the RGC by immunoprecipitating the complex from 293A cells. In these cells, the complex exists in a largely unphosphorylated state, as determined by blotting the RGC immunoprecipitation with the pAS antibody (Fig. 3*E*, *pAS blot*). Immunoprecipitated RGC was phosphorylated *in vitro* by incubating with recombinant His-Akt2 and binding to 14-3-3 was then assessed by overlay assay. 14-3-3 did not bind to either subunit of the RGC in the absence of His-Akt2 (Fig. 3*E*, *fourth lane*). 14-3-3 bound to RGC2 after incubation with His-Akt2, although the kinase phosphorylated both RGC1 and RGC2 in an *in vitro* setting (Fig. 3*E*, *fifth lane*). These data are consistent with our previous data showing that 14-3-3 binding to the complex requires RGC2 (Fig. 2, *E* and *F*). Finally, decreasing phosphorylation of the complex by treating the immunoprecipitated proteins with calf intestinal phosphatase (*CIP*) after incubation with His-Akt2 reduced the binding between 14-3-3 and RGC2 (Fig. 3*E*, *sixth lane*). Together, these data show that Akt-catalyzed phosphorylation of RGC2 is necessary and sufficient for recognition of the complex by 14-3-3.

Akt phosphorylates RGC2 on at least three serine/threonine residues (20, 40). Previous studies demonstrated that 14-3-3 binding can block phosphorylated residues from dephosphorylation by phosphatases (41). Thus, we designed a phosphatase protection assay that exploits this property to identify potential 14-3-3 recognition sites on RGC2 (Fig. 4*A*). The RGC was overexpressed and then immunoprecipitated from 293T cells, which contain high levels of active Akt. As is evident in Fig. 4*B*, RGC2 is highly phosphorylated in these cells. The isolated complex was bound to recombinant GST-14-3-3 *in vitro* and then treated with λ-phosphatase for increasing amounts of time. The ability of λ-phosphatase to dephosphorylate RGC2 residues was assessed by Western blotting with the pAS antibody and site-specific RGC2 phospho-antibodies (Fig. 4*B*). When immunoprecipitated RGC was treated with λ-phosphatase but not preincubated with GST-14-3-3, the phosphatase completely dephosphorylated serines 486 and 696 and greatly reduced phosphorylation of threonine 715 by as soon as 2 min after treatment (Fig. 4*B*). However, when the immunoprecipitated proteins were bound to GST-14-3-3 before the addition of λ-phosphatase, dephosphorylation of threonine 715 was significantly blocked up to 30 min after addition of the enzyme. In contrast, serines 486 and 696 were still completely dephosphorylated after 2 min of λ-phosphatase treatment. These data suggest that 14-3-3 may bind to the RGC through phospho-threonine 715 on RGC2. However, this assay alone did not rule out other possibilities, such as a decreased accessibility of this site to λ-phosphatase in the presence of 14-3-3, perhaps because of a change in the conformation of the protein or because 14-3-3 physically blocks access to this site without directly binding to it.

To directly test whether threonine 715 is necessary for recognition of the complex by 14-3-3, we mutated this residue to a non-phosphorylatable alanine residue. Wild-type RGC1/2 and RGC1/2^{T715A} were expressed at comparable levels in 293T cells and analyzed for their ability to directly interact with GST-14-3-3 in an *in vitro* setting using an overlay assay (Fig. 4*C*). GST-14-3-3 bound to wild-type RGC2 in this assay but failed to interact with RGC2^{T715A}, demonstrating that this residue is indeed required for recognition of RGC2 by 14-3-3. Interaction between 14-3-3 and the complex in cells was assessed by pull-down assay (Fig. 4*D*). GST-14-3-3 pulled down wild-type RGC1/2, consistent with our previous results (Figs. 2*F* and 3, *A–D*). The amount of RGC1/2^{T715A} that interacted with GST-14-3-3 was $<$ 10% of that of the wild type, again demonstrating that threonine 715 is required for 14-3-3 to bind to the complex. Residual binding may be due to nonspecific interactions between the RGC and 14-3-3, or it could indicate that there are other sites within the complex that can weakly coordinate binding. Together, these data demonstrate that 14-3-3 recognizes and binds to the RGC through phosphorylated threonine 715 on RGC2.

14-3-3 Binding Inhibits the RalGAP Complex GAP Function—We showed previously that Akt-catalyzed phosphorylation inhibits the RalGAP complex through an unknown mechanism (20). There are many examples of 14-3-3 acting in signaling pathways by binding to and modulating the function of its target proteins (42). Thus, we hypothesized that Akt inhibits the RGC by increasing its recognition by 14-3-3 proteins. To assess whether 14-3-3 binding is involved in RGC inhibition, we first tested the effect of this protein on the catalytic activity of the complex by performing *in vitro* GAP assays. RGC expressed in 293A cells was immunoprecipitated, mock-treated, or phosphorylated *in vitro* with recombinant His-Akt2 and then bound to recombinant GST-14-3-3. Consistent with previous studies, immunoprecipitated RGC enhanced GTP hydrolysis on recombinant RalA, and Akt-catalyzed phosphorylation of the complex had no effect on its *in vitro* activity (20, 21) (Fig. 5*A*). Incubation of the unphosphorylated complex or the phosphorylated complex with GST-14-3-3 did not affect its *in vitro* GAP activity, suggesting that 14-3-3 does not directly inhibit the catalytic activity of the RGC. We also tested the effect of 14-3-3 on the complex by comparing the *in vitro* GAP activity of immunoprecipitated wild-type RGC1/2 and RGC1/2^{T715A} expressed

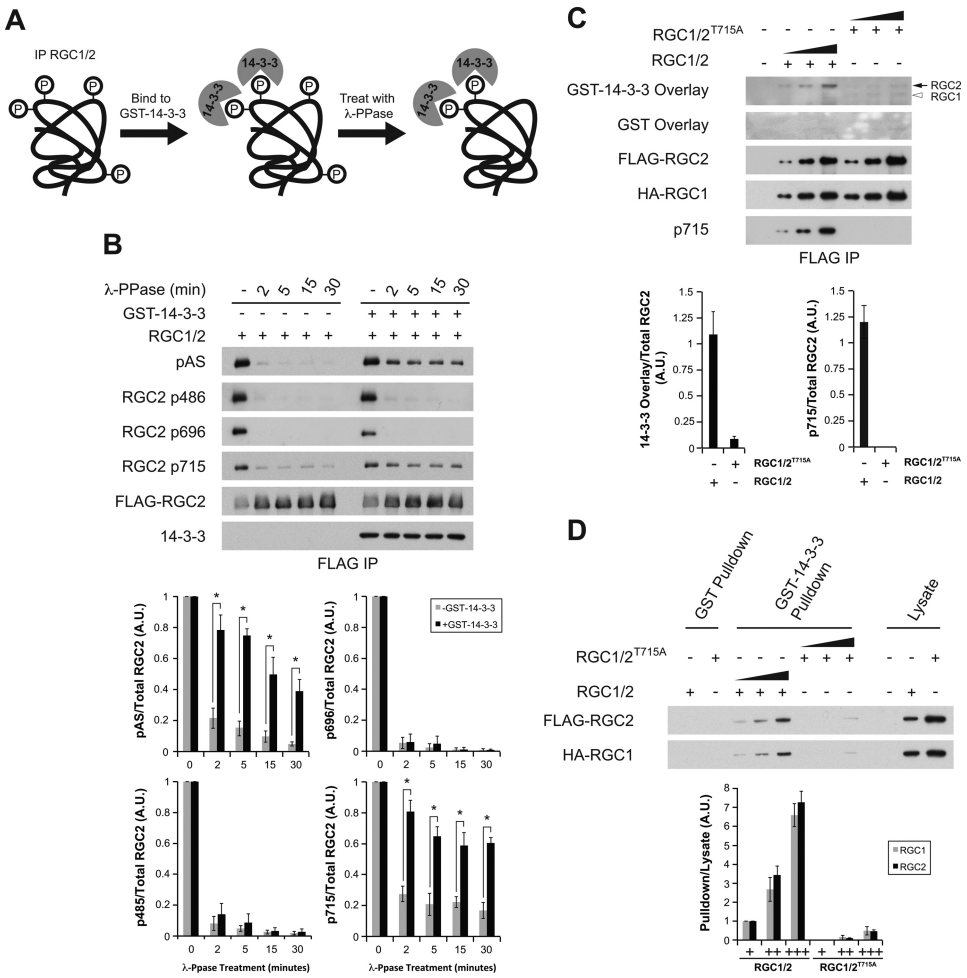

FIGURE 4. **RGC2^{T715} phosphorylation is required for 14-3-3 binding.** *A*, schematic of λ-phosphatase protection assay. *IP*, immunoprecipitation. *B*, λ-phosphatase protection assay. 293T cells were transfected with empty vector or HA-RGC1 and FLAG-RGC2. Two days after transfection, cells were lysed, and the RGC was immunoprecipitated from lysates using an anti-FLAG antibody. The immune complexes were then incubated with or without GST-14-3-3 for 1 h. After removal of unbound GST-14-3-3, the immunoprecipitated proteins were incubated with λ-phosphatase for the indicated periods of time. Immune complexes were separated by SDS-PAGE. Total RGC2 levels, 14-3-3 binding, and RGC2 phosphorylation were assessed by Western blot analysis with the indicated antibodies. *Top panel*, Western blot analysis. *Bottom panel*, phospho-RGC2 and total FLAG-RGC2 signals were quantified and normalized to signals in the absence of λ-phosphatase. Normalized phospho-RGC2/total RGC2 ratios are presented as the mean ± S.E. from three independent experiments. *, $p < 0.02$, Student's *t* test. *A.U.*, arbitrary unit. *C*, 293T cells were transfected with HA-RGC1 and wild-type FLAG-RGC2 or FLAG-RGC2^{T715A} as indicated. Two days after transfection, the RGC was immunoprecipitated from cell lysates using an anti-FLAG antibody. Increasing amounts of immune complexes were resolved by SDS-PAGE followed by Western blot analysis with the indicated antibodies. 14-3-3 binding to wild-type RGC2 or RGC2^{T715A} was assessed by overlay using DIG-labeled GST or GST-14-3-3 followed by incubation with anti-DIG HRP antibody. The relative positions of HA-RGC1 and FLAG-RGC2 are indicated by an *arrowhead* and *arrow*, respectively. *Top panel*, Western blot analysis. *Bottom panel*, the GST-14-3-3 overlay, p715, and FLAG-RGC2 signals were quantified, and the ratio of 14-3-3 overlay/total RGC2 and p715/total RGC2 ratios were calculated. *Error bars* represent mean ± S.E. of two independent experiments. *D*, 293T cells were transfected with HA-RGC1 and wild-type FLAG-RGC2 or FLAG-RGC2^{T715A} as indicated. Two days after transfection, cleared cell lysates were incubated with immobilized GST or GST-14-3-3. Lysates and increasing amounts of the pull-down were resolved by SDS-PAGE. The amount of wild-type RGC1/2 and RGC1/2^{T715A} bound to 14-3-3 was assessed by Western blot analysis with the indicated antibodies. *Top panel*, Western blot analysis. *Bottom panel*, RGC1 and RGC2 signals in the pull-downs and lysates were quantified and normalized to the signal in the *third lane*. The normalized pull-down/lysate ratio is presented at mean ± S.E. of two independent experiments.

in 293T cells. Both the wild-type and mutant complexes accelerated GTP hydrolysis on RalA to the same extent, providing further evidence that 14-3-3 does not affect catalytic activity (Fig. 5*B*).

To test whether 14-3-3 binding altered the function of the complex in cells, we first explored the effect of dominant-negative 14-3-3 (14-3-3 DN), a mutant form of the protein that dimerizes with endogenous 14-3-3 and blocks binding to target phosphorylated proteins, on RalA activity. 14-3-3 DN decreased binding between 14-3-3 and the RGC in a dose-dependent manner without affecting phosphorylation of threonine 715 (Fig. 6, *A* and *B*). Thus, expression of this construct allowed us to examine the role of 14-3-3 binding independent of the phosphorylation state of the complex. Overexpression of 14-3-3 DN in 293T cells, in which endogenous RGC2 expression is undetectable, had no effect on Ral activity, as determined by a pull-down assay using the Ral binding domain of the Ral effector protein RalBP1 (Fig. 6*B*, compare *first* and *second lanes*). As expected, overexpression of the wild-type RGC decreased RalA activation by 54% (Fig. 6*B*, *third lane*). Introduction of both wild-type RGC and 14-3-3 DN further decreased levels of active RalA (Fig. 6*B*, *fourth lane*), suggesting that 14-3-3 binding does, indeed, inhibit the complex in cells. Furthermore, because this effect of 14-3-3 DN was only

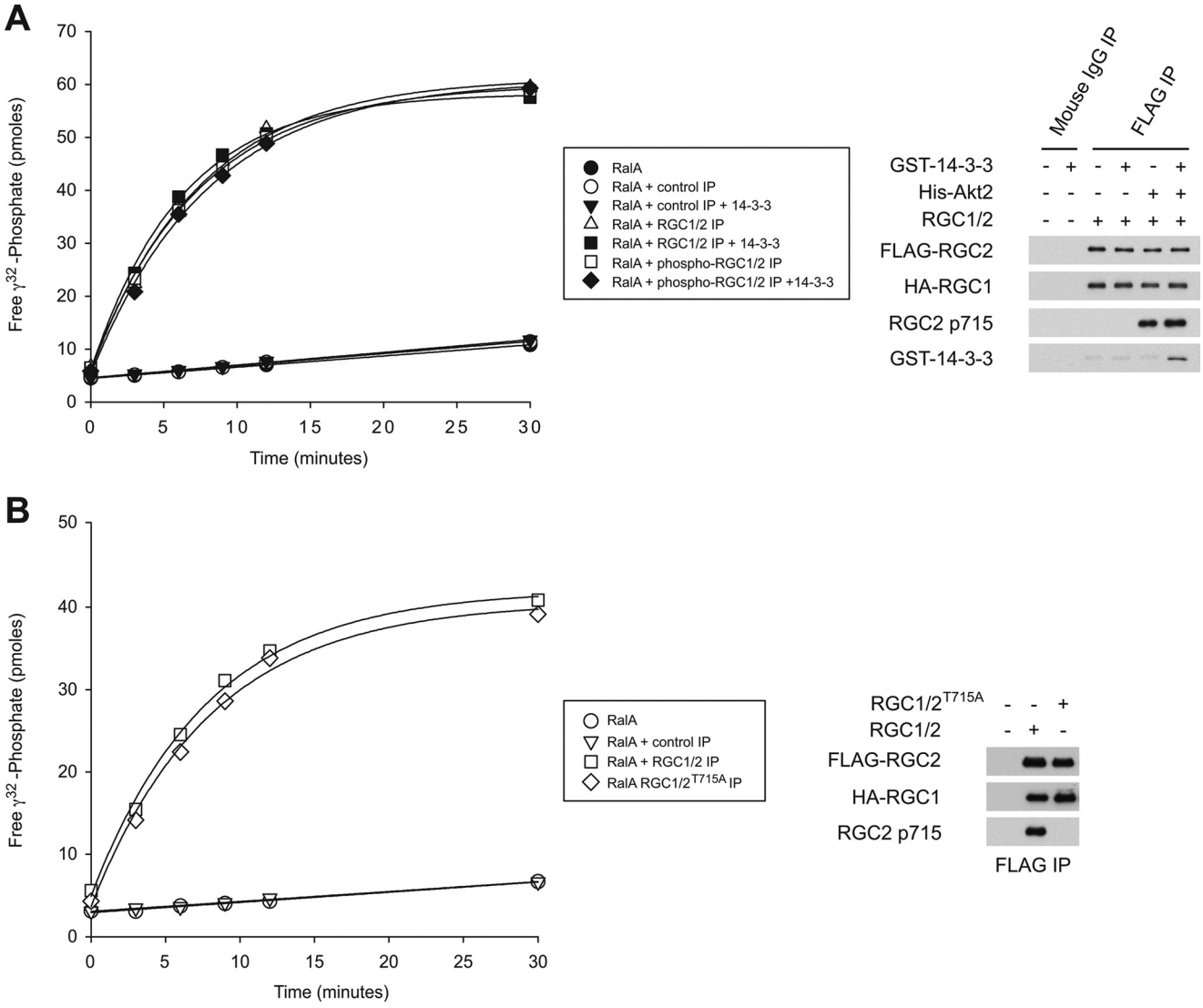

FIGURE 5. **14-3-3 binding does not affect RalGAP complex *in vitro* catalytic activity.** *A*, 293A cells were transfected with empty vector or HA-RGC1 and FLAG-RGC2 as indicated. Two days after transfection, cell lysates were subjected to immunoprecipitation (*IP*) using a control antibody or anti-FLAG antibody. Immune complexes were then incubated with ATP and His-Akt2 as indicated. After removal of the kinase, immune complexes were incubated with GST-14-3-3 for 1 h. *In vitro* GAP activity was then determined by incubating the immune complexes with recombinant GST-RalA loaded with [γ^{32}]GTP. Free γ^{32} phosphate was measured at the indicated times as a reflection of GTP hydrolysis. *Right panel*, immune complexes were resolved by SDS-PAGE and analyzed by Western blotting with the indicated antibodies. *B*, 293T cells were transfected with HA-RGC1 and wild-type FLAG-RGC2 or FLAG-RGC2^{T715A} as indicated. Two days after transfection, the RGC was immunoprecipitated from lysates using an anti-FLAG antibody. GAP activity was analyzed by *in vitro* GAP assay as described in *A*. *Right panel*, RGC1/2 complexes present in the assay were determined by Western blot analysis with the indicated antibodies.

observed upon expression of the RGC, these data suggest that 14-3-3 acts primarily through the RGC rather than other Ral regulatory proteins to modulate RalA activity. Because 14-3-3 recognizes the complex through phosphorylated threonine 715 (Fig. 4, *A–D*), the effect of 14-3-3 DN on phosphorylation-deficient RGC1/2^{T715A} was also tested. In this case, overexpression of 14-3-3 DN had no further effect on RalA activity (Fig. 6*C*).

Finally, we directly compared the RalGAP activity of wild-type RGC1/2 and RGC1/2^{T715A}. At low and high doses, RGC1/2^{T715A} displayed a higher activity in cells than the wild-type complex, as evidenced by a greater inhibition of RalA (Fig. 6*D*). Together, these data establish a novel role for 14-3-3 as a component of the regulatory machinery that modulates RalA activity in cells by decreasing the RalGAP function of the RGC upon Akt-catalyzed phosphorylation.

DISCUSSION

Signaling pathways regulate many cellular processes by modulating small GTPase activity. Although signaling proteins can in some cases exert direct effects on small GTPases through phosphorylation (43–46), they often indirectly regulate this family of proteins by acting on GEFs and GAPs. Thus, GEFs and GAPs translate upstream signals into biological outputs through the control of small GTPase activity. One example of this is PI3-kinase signaling, which activates RalA by regulating Ral GEFs and GAPs (20, 47). We showed previously that in adipocytes, the RGC acts as an important regulatory module that suppresses RalA activity in the absence of insulin. Stimulation with the hormone results in Akt-catalyzed inhibitory phosphorylation of the RGC and, in turn, elevated RalA activity, Glut4 exocytosis, and glucose uptake (7, 20). Although the role

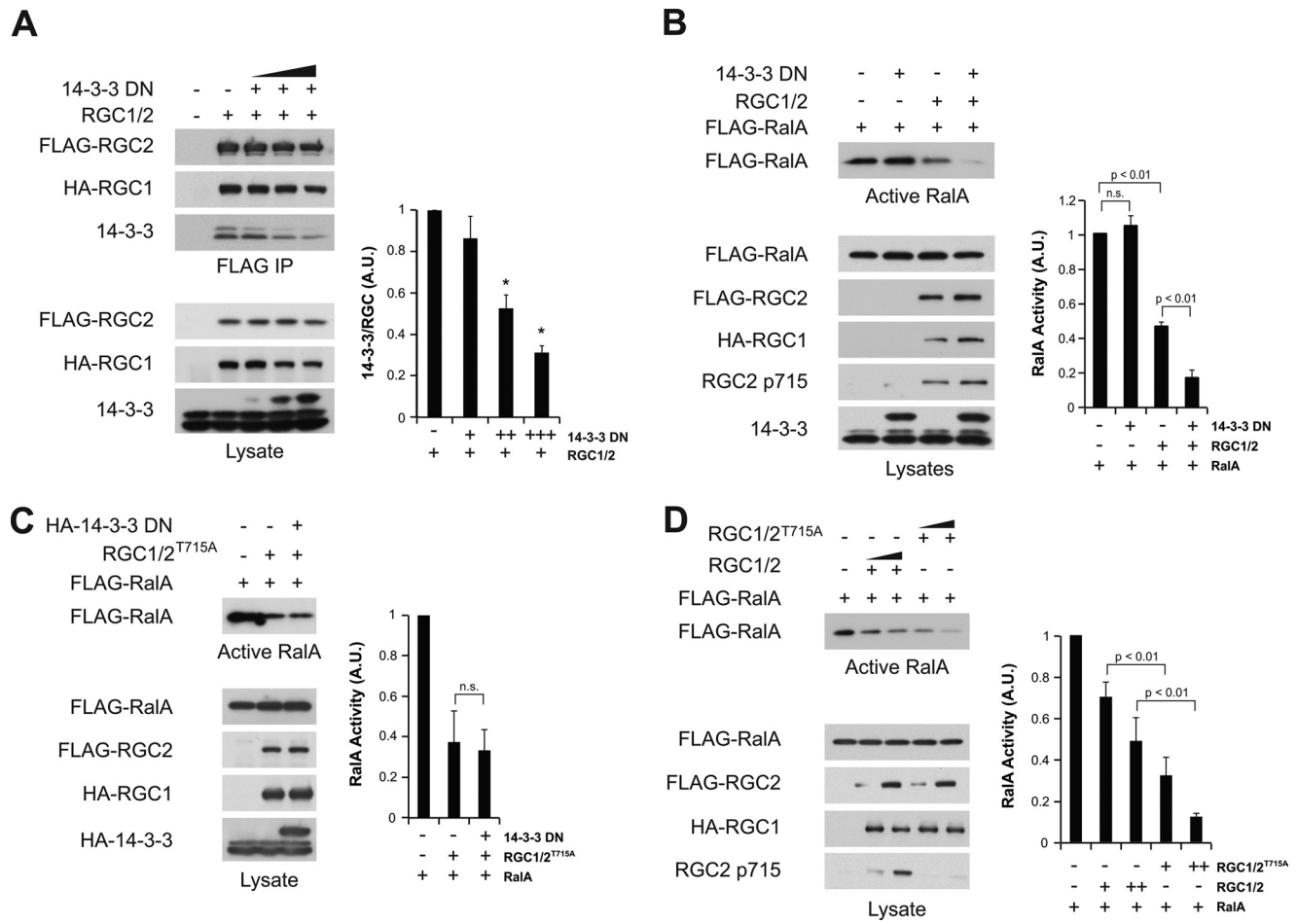

FIGURE 6. **14-3-3 binding inhibits the RalGAP complex in cells.** *A*, 293T cells were transfected with a constant amount of HA-RGC1/FLAG-RGC2 and increasing amounts of dominant-negative HA-14-3-3 (HA-14-3-3 DN). Two days after transfection, the RGC was immunoprecipitated from cell lysates using an anti-FLAG antibody. Cell lysates and immune complexes were resolved by SDS-PAGE. Levels of overexpressed proteins and binding between the RGC and endogenous 14-3-3 were determined by Western blotting with the indicated antibodies. *Left panel*, Western blot analysis. *Right panel*, 14-3-3 and HA-RGC2 signals in the FLAG immunoprecipitations were quantified and normalized to signals in the absence of 14-3-3 DN. The normalized 14-3-3/RGC2 ratio is presented as the mean ± S.E. of three independent experiments. *, $p < 0.03$, Student's *t* test. *A.U.*, arbitrary unit. *B*, 293T cells were transfected with FLAG-RalA, HA-RGC1, wild-type FLAG-RGC2, and HA-14-3-3 DN as indicated. Two days after transfection, active RalA was detected by incubating cell lysates with GST-RalBP1 Ral binding domain bound to glutathione beads. Lysates and pull-downs were resolved by SDS-PAGE and Western blot analysis with the indicated antibodies. *Left panel*, Western blot analysis. *Right panel*, the RalA signal in the pull-down and lysates was quantified and normalized to the *first lane*. Normalized RalA activity (pull-down/total RalA) is presented as the mean ± S.E. of three independent experiments. Statistical significance was determined by Student's *t* test. *n.s.*, not significant. *C*, 293T cells were transfected with FLAG-RalA, HA-RGC1, FLAG-RGC2^{T715A}, and HA-14-3-3 DN as indicated. Active RalA levels were determined as in *B*. *Left panel*, Western blot analysis. *Right panel*, RalA activity was quantified as described in *B*. *Error bars* represent mean ± S.E. Statistical significance was determined by Student's *t* test. *D*, 293T cells were transfected with FLAG-RalA, HA-RGC1, wild-type FLAG-RGC2, or FLAG-RGC2^{T715A} as indicated. Active RalA levels were determined as in *B*. *Left panel*, Western blot analysis. *Right panel*, RalA activity was quantified as described in *B*. *Error bars* represent mean ± S.E. Statistical significance was determined by Student's *t* test.

of the RGC in other cellular contexts has not yet been explored, the ubiquitous expression of this protein complex suggests that it likely plays a larger function as a regulator of RalA.

Although phosphorylation of the RGC is known to inhibit its activity, the mechanism for inhibition is currently unclear. Phosphorylation can regulate GEF and GAP function in various ways, including by altering catalytic activity, localization, protein conformation, and binding partners (48). In some instances, phosphorylation modulates the function of GAPs and GEFs by increasing their interaction with 14-3-3 proteins. Additionally, 14-3-3s recognize a vast network of proteins in response to insulin to coordinate changes in energy uptake and use (49). Among these 14-3-3 targets are the RabGAP AS160, which plays a role in glucose uptake (50), and the RhebGAP TSC2, which controls protein synthesis through the TORC1 complex (24, 25). For both AS160 and TSC2, Akt-catalyzed phosphorylation of the GAP increases its association with and inhibition by 14-3-3 (29, 36). These examples suggest that insulin may initiate an anabolic program in part by activating multiple small GTPases through a common mechanism involving 14-3-3-mediated inhibition of GAPs.

In this study, we showed that, similar to TSC2 and AS160, 14-3-3 binds to the phosphorylated RGC. 14-3-3 recognizes the catalytic subunit of the complex, RGC2, through threonine 715, a site that we previously showed is phosphorylated by Akt (20). Indeed, 14-3-3·RGC complex formation is dependent on threonine 715 phosphorylation, as mutation of this residue to a non-phosphorylatable alanine residue blocked the interaction between RGC2 and 14-3-3. Furthermore, 14-3-3 docking to RGC2 appears to inhibit GAP function in cells, as blocking the

association between 14-3-3 and RGC2 either by overexpression of dominant-negative 14-3-3 or by T715A mutation resulted in enhanced suppression of active RalA levels. Our data suggest that 14-3-3 primarily acts through the RGC to regulate RalA GTP loading. However, we cannot completely rule out the role of other Ral regulators that may interact with 14-3-3.

Although these studies provide further insight into the mechanisms governing RalA regulation by the RGC in cells, several outstanding questions remain. In particular, how does 14-3-3 inhibit RGC function? In agreement with our previous studies suggesting that phosphorylation does not directly alter catalytic activity (20), 14-3-3 binding to the complex does not affect *in vitro* GAP activity. For both AS160 and TSC2, it was originally hypothesized that 14-3-3 alters their cellular localization and, in doing so, decreases their interaction with target G proteins. However, although multiple groups have reported that AS160 dissociates from Glut4-containing vesicles upon phosphorylation, this dissociation does not appear to be necessary for inhibition of the GAP function by 14-3-3, suggesting that 14-3-3 may affect this GAP in other ways (51, 52). There is some experimental evidence to support a role for 14-3-3 in partitioning TSC2 away from membranes that contain Rheb rather than affecting catalytic activity (35). In the case of the RGC, Akt-catalyzed phosphorylation decreases its interaction with RalA (20). However, we have not been able to detect a change in the subcellular localization of the RGC because of either phosphorylation or 14-3-3 binding by either subcellular fractionation or immunofluorescence[3]. Future studies are needed to further elucidate the precise role of 14-3-3s in modulating the activity and association of these GAPs with their target small GTPases. Nevertheless, these findings establish 14-3-3 as a component of the regulatory machinery controlling RalA activity in cells and further support a common mechanism for regulation of GAPs downstream of PI3-kinase/Akt signaling.

Acknowledgments—We thank Dr. Ken Inoki for kindly sharing reagents and members of the Saltiel laboratory for insightful discussions.

REFERENCES

1. Chien, Y., and White, M. A. (2003) RAL GTPases are linchpin modulators of human tumour-cell proliferation and survival. *EMBO Rep.* **4,** 800–806
2. Lim, K. H., O'Hayer, K., Adam, S. J., Kendall, S. D., Campbell, P. M., Der, C. J., and Counter, C. M. (2006) Divergent roles for RalA and RalB in malignant growth of human pancreatic carcinoma cells. *Curr. Biol.* **16,** 2385–2394
3. Rossé, C., Hatzoglou, A., Parrini, M. C., White, M. A., Chavrier, P., and Camonis, J. (2006) RalB mobilizes the exocyst to drive cell migration. *Mol. Cell Biol.* **26,** 727–734
4. Ohta, Y., Suzuki, N., Nakamura, S., Hartwig, J. H., and Stossel, T. P. (1999) The small GTPase RalA targets filamin to induce filopodia. *Proc. Natl. Acad. Sci. U.S.A.* **96,** 2122–2128
5. Jullien-Flores, V., Dorseuil, O., Romero, F., Letourneur, F., Saragosti, S., Berger, R., Tavitian, A., Gacon, G., and Camonis, J. H. (1995) Bridging Ral GTPase to Rho pathways. RLIP76, a Ral effector with CDC42/Rac GTPase-activating protein activity. *J. Biol. Chem.* **270,** 22473–22477
6. van Dam, E. M., and Robinson, P. J. (2006) Ral. mediator of membrane trafficking. *Int. J. Biochem. Cell Biol.* **38,** 1841–1847
7. Chen, X. W., Leto, D., Chiang, S. H., Wang, Q., and Saltiel, A. R. (2007) Activation of RalA is required for insulin-stimulated Glut4 trafficking to the plasma membrane via the exocyst and the motor protein Myo1c. *Dev. Cell* **13,** 391–404
8. Maehama, T., Tanaka, M., Nishina, H., Murakami, M., Kanaho, Y., and Hanada, K. (2008) RalA functions as an indispensable signal mediator for the nutrient-sensing system. *J. Biol. Chem.* **283,** 35053–35059
9. Xu, L., Salloum, D., Medlin, P. S., Saqcena, M., Yellen, P., Perrella, B., and Foster, D. A. (2011) Phospholipase D mediates nutrient input to mammalian target of rapamycin complex 1 (mTORC1). *J. Biol. Chem.* **286,** 25477–25486
10. Traut, T. W. (1994) Physiological concentrations of purines and pyrimidines. *Mol. Cell Biochem.* **140,** 1–22
11. Ferro, E., and Trabalzini, L. (2010) RalGDS family members couple Ras to Ral signalling and that's not all. *Cell. Signal.* **22,** 1804–1810
12. Matsubara, K., Kishida, S., Matsuura, Y., Kitayama, H., Noda, M., and Kikuchi, A. (1999) Plasma membrane recruitment of RalGDS is critical for Ras-dependent Ral activation. *Oncogene* **18,** 1303–1312
13. Kishida, S., Koyama, S., Matsubara, K., Kishida, M., Matsuura, Y., and Kikuchi, A. (1997) Colocalization of Ras and Ral on the membrane is required for Ras-dependent Ral activation through Ral GDP dissociation stimulator. *Oncogene* **15,** 2899–2907
14. Takaya, A., Kamio, T., Masuda, M., Mochizuki, N., Sawa, H., Sato, M., Nagashima, K., Mizutani, A., Matsuno, A., Kiyokawa, E., and Matsuda, M. (2007) R-Ras regulates exocytosis by Rgl2/Rlf-mediated activation of RalA on endosomes. *Mol. Biol. Cell* **18,** 1850–1860
15. Rebhun, J. F., Chen, H., and Quilliam, L. A. (2000) Identification and characterization of a new family of guanine nucleotide exchange factors for the ras-related GTPase Ral. *J. Biol. Chem.* **275,** 13406–13410
16. Hernandez-Muñoz, I., Malumbres, M., Leonardi, P., and Pellicer, A. (2000) The Rgr oncogene (homologous to RalGDS) induces transformation and gene expression by activating Ras, Ral and Rho mediated pathways. *Oncogene* **19,** 2745–2757
17. Gotoh, T., Cai, D., Tian, X., Feig, L. A., and Lerner, A. (2000) p130Cas regulates the activity of AND-34, a novel Ral, Rap1, and R-Ras guanine nucleotide exchange factor. *J. Biol. Chem.* **275,** 30118–30123
18. Cascone, I., Selimoglu, R., Ozdemir, C., Del Nery, E., Yeaman, C., White, M., and Camonis, J. (2008) Distinct roles of RalA and RalB in the progression of cytokinesis are supported by distinct RalGEFs. *EMBO J.* **27,** 2375–2387
19. Emkey, R., Freedman, S., and Feig, L. A. (1991) Characterization of a GTPase-activating protein for the Ras-related Ral protein. *J. Biol. Chem.* **266,** 9703–9706
20. Chen, X. W., Leto, D., Xiong, T., Yu, G., Cheng, A., Decker, S., and Saltiel, A. R. (2011) A Ral GAP complex links PI 3-kinase/Akt signaling to RalA activation in insulin action. *Mol. Biol. Cell* **22,** 141–152
21. Shirakawa, R., Fukai, S., Kawato, M., Higashi, T., Kondo, H., Ikeda, T., Nakayama, E., Okawa, K., Nureki, O., Kimura, T., Kita, T., and Horiuchi, H. (2009) Tuberous sclerosis tumor suppressor complex-like complexes act as GTPase-activating proteins for Ral GTPases. *J. Biol. Chem.* **284,** 21580–21588
22. Csépányi-Kömi, R., Lévay, M., and Ligeti, E. (2012) Small G proteins and their regulators in cellular signalling. *Mol. Cell Endocrinol.* **353,** 10–20
23. Garami, A., Zwartkruis, F. J., Nobukuni, T., Joaquin, M., Roccio, M., Stocker, H., Kozma, S. C., Hafen, E., Bos, J. L., and Thomas, G. (2003) Insulin activation of Rheb, a mediator of mTOR/S6K/4E-BP signaling, is inhibited by TSC1 and 2. *Mol. Cell* **11,** 1457–1466
24. Inoki, K., Li, Y., Xu, T., and Guan, K. L. (2003) Rheb GTPase is a direct target of TSC2 GAP activity and regulates mTOR signaling. *Genes Dev.* **17,** 1829–1834
25. Potter, C. J., Pedraza, L. G., and Xu, T. (2002) Akt regulates growth by directly phosphorylating Tsc2. *Nat. Cell Biol.* **4,** 658–665
26. Chen, X. W., and Saltiel, A. R. (2011) Ral's engagement with the exocyst. Breaking up is hard to do. *Cell Cycle* **10,** 2299–2304
27. Bernards, A., and Settleman, J. (2004) GAP control. Regulating the regulators of small GTPases. *Trends Cell Biol.* **14,** 377–385
28. Feng, L., Yunoue, S., Tokuo, H., Ozawa, T., Zhang, D., Patrakitkomjorn, S., Ichimura, T., Saya, H., and Araki, N. (2004) PKA phosphorylation and 14-3-3 interaction regulate the function of neurofibromatosis type I tumor

suppressor, neurofibromin. *FEBS Lett.* **557,** 275–282
29. Li, Y., Inoki, K., Yeung, R., and Guan, K. L. (2002) Regulation of TSC2 by 14-3-3 binding. *J. Biol. Chem.* **277,** 44593–44596
30. O'Toole, T. E., Bialkowska, K., Li, X., and Fox, J. E. (2011) Tiam1 is recruited to β1-integrin complexes by 14-3-3ζ where it mediates integrin-induced Rac1 activation and motility. *J. Cell Physiol.* **226,** 2965–2978
31. Yaffe, M. B., Rittinger, K., Volinia, S., Caron, P. R., Aitken, A., Leffers, H., Gamblin, S. J., Smerdon, S. J., and Cantley, L. C. (1997) The structural basis for 14-3-3:phosphopeptide binding specificity. *Cell* **91,** 961–971
32. Liu, J., DeYoung, S. M., Zhang, M., Zhang, M., Cheng, A., and Saltiel, A. R. (2005) Changes in integrin expression during adipocyte differentiation. *Cell Metab.* **2,** 165–177
33. Inoue, M., Chiang, S. H., Chang, L., Chen, X. W., and Saltiel, A. R. (2006) Compartmentalization of the exocyst complex in lipid rafts controls Glut4 vesicle tethering. *Mol. Biol. Cell* **17,** 2303–2311
34. Liu, J., Wu, J., Oliver, C., Shenolikar, S., and Brautigan, D. L. (2000) Mutations of the serine phosphorylated in the protein phosphatase-1-binding motif in the skeletal muscle glycogen-targeting subunit. *Biochem. J.* **346,** 77–82
35. Cai, S. L., Tee, A. R., Short, J. D., Bergeron, J. M., Kim, J., Shen, J., Guo, R., Johnson, C. L., Kiguchi, K., and Walker, C. L. (2006) Activity of TSC2 is inhibited by AKT-mediated phosphorylation and membrane partitioning. *J. Cell Biol.* **173,** 279–289
36. Ramm, G., Larance, M., Guilhaus, M., and James, D. E. (2006) A role for 14-3-3 in insulin-stimulated GLUT4 translocation through its interaction with the RabGAP AS160. *J. Biol. Chem.* **281,** 29174–29180
37. Datta, S. R., Katsov, A., Hu, L., Petros, A., Fesik, S. W., Yaffe, M. B., and Greenberg, M. E. (2000) 14-3-3 proteins and survival kinases cooperate to inactivate BAD by BH3 domain phosphorylation. *Mol. Cell* **6,** 41–51
38. Palmer, D., Jimmo, S. L., Raymond, D. R., Wilson, L. S., Carter, R. L., and Maurice, D. H. (2007) Protein kinase A phosphorylation of human phosphodiesterase 3B promotes 14-3-3 protein binding and inhibits phosphatase-catalyzed inactivation. *J. Biol. Chem.* **282,** 9411–9419
39. Hurd, T. W., Fan, S., Liu, C. J., Kweon, H. K., Hakansson, K., and Margolis, B. (2003) Phosphorylation-dependent binding of 14-3-3 to the polarity protein Par3 regulates cell polarity in mammalian epithelia. *Curr. Biol.* **13,** 2082–2090
40. Gridley, S., Lane, W. S., Garner, C. W., and Lienhard, G. E. (2005) Novel insulin-elicited phosphoproteins in adipocytes. *Cell. Signal.* **17,** 59–66
41. Dougherty, M. K., and Morrison, D. K. (2004) Unlocking the code of 14-3-3. *J. Cell Sci.* **117,** 1875–1884
42. Fu, H., Subramanian, R. R., and Masters, S. C. (2000) 14-3-3 proteins. Structure, function, and regulation. *Annu. Rev. Pharmacol. Toxicol.* **40,** 617–647
43. Lim, K. H., Brady, D. C., Kashatus, D. F., Ancrile, B. B., Der, C. J., Cox, A. D., and Counter, C. M. (2010) Aurora-A phosphorylates, activates, and relocalizes the small GTPase RalA. *Mol. Cell Biol.* **30,** 508–523
44. Alan, J. K., Berzat, A. C., Dewar, B. J., Graves, L. M., and Cox, A. D. (2010) Regulation of the Rho family small GTPase Wrch-1/RhoU by C-terminal tyrosine phosphorylation requires Src. *Mol. Cell Biol.* **30,** 4324–4338
45. Riento, K., Totty, N., Villalonga, P., Garg, R., Guasch, R., and Ridley, A. J. (2005) RhoE function is regulated by ROCK I-mediated phosphorylation. *EMBO J.* **24,** 1170–1180
46. Bivona, T. G., Quatela, S. E., Bodemann, B. O., Ahearn, I. M., Soskis, M. J., Mor, A., Miura, J., Wiener, H. H., Wright, L., Saba, S. G., Yim, D., Fein, A., Pérez de Castro, I., Li, C., Thompson, C. B., Cox, A. D., and Philips, M. R. (2006) PKC regulates a farnesyl-electrostatic switch on K-Ras that promotes its association with Bcl-XL on mitochondria and induces apoptosis. *Mol. Cell* **21,** 481–493
47. Tian, X., Rusanescu, G., Hou, W., Schaffhausen, B., and Feig, L. A. (2002) PDK1 mediates growth factor-induced Ral-GEF activation by a kinase-independent mechanism. *EMBO J.* **21,** 1327–1338
48. Bos, J. L., Rehmann, H., and Wittinghofer, A. (2007) GEFs and GAPs. Critical elements in the control of small G proteins. *Cell* **129,** 865–877
49. Chen, S., Synowsky, S., Tinti, M., and MacKintosh, C. (2011) The capture of phosphoproteins by 14-3-3 proteins mediates actions of insulin. *Trends Endocrinol. Metab.* **22,** 429–436
50. Sano, H., Kane, S., Sano, E., Miinea, C. P., Asara, J. M., Lane, W. S., Garner, C. W., and Lienhard, G. E. (2003) Insulin-stimulated phosphorylation of a Rab GTPase-activating protein regulates GLUT4 translocation. *J. Biol. Chem.* **278,** 14599–14602
51. Stöckli, J., Davey, J. R., Hohnen-Behrens, C., Xu, A., James, D. E., and Ramm, G. (2008) Regulation of glucose transporter 4 translocation by the Rab guanosine triphosphatase-activating protein AS160/TBC1D4. Role of phosphorylation and membrane association. *Mol. Endocrinol.* **22,** 2703–2715
52. Larance, M., Ramm, G., Stöckli, J., van Dam, E. M., Winata, S., Wasinger, V., Simpson, F., Graham, M., Junutula, J. R., Guilhaus, M., and James, D. E. (2005) Characterization of the role of the Rab GTPase-activating protein AS160 in insulin-regulated GLUT4 trafficking. *J. Biol. Chem.* **280,** 37803–37813